Available online at www.CivileJournal.org

Civil Engineering Journal

(E-ISSN: 2476-3055; ISSN: 2676-6957)

Vol. 8, No. 10, October, 2022

Experimental and Numerical Study on the Composite Column Behavior: Loess Soil Reinforced by Concrete-Stone Column

Mahmood A. Salam [1], Qiyao Wang [1*], Jinbo Huang [1]

[1] *School of Civil Engineering, Chang'an University, Xi'an, 710000, China.*

Received 26 May 2022; Revised 12 September 2022; Accepted 23 September 2022; Published 01 October 2022

Abstract

Stone columns are an effective approach to improving the bearing capacity of weak soils, which has led to increased interest in the improved soil method being further developed and expanded. In addition, enhancing the bearing capacity of stone columns has recently received great attention. This paper studies the effects of embedded concrete parts on the stone columns' bearing capacity and bulging failure. Moreover, arranging solutions to the problem of bulging failure and reduced bearing capacity of stone columns and understanding the stone columns' failure after reinforcement by comparing the results. Stone columns are either embedded in a solid concrete part or unreinforced were examined using large-scale laboratory experiments, and numerical simulation was performed using ABAQUS. The models test with a scale factor of 1:7 was employed. The results demonstrated that using a concrete part on the top of the stone column greatly increases its bearing capacity and the efficiency of the surrounding soil. Concrete-stone columns (CSCs) show stress concentration ratio (n) enhancement and significant resistance to bulging failure deformation. The concrete-stone column shows an enhancement related to increasing the concrete part length; also, the CSCs stiffness increases the surrounding loess soil capacity. The horizontal stresses of CSCs demonstrate the type of column failure behavior; the column may fail due to shear stress in a long concrete part case.

Keywords: Stone Column; Concrete-Stone Column; Bulging; Stress Concentration Ratio; Loess Soil; ABAQUS.

1. Introduction

The complications associated with soft soil have been the primary challenge to infrastructure planning and implementation. The potential use of stone columns (also generally referred to as granular piles) has many advantages, such as cost-effective and environmentally friendly methods. Further, stone columns are typically applied to improve the bearing capacity, and reduce the differential and total settlements. They accelerate the soil consolidation and enhance its stability; the stone columns' stiffness decreases vertical stress on the soil. Geotechnical Engineers use the stone columns to force the ground to adopt the project's specifications by modifying the soil's natural state instead of modifying the design within the ground's natural state limitations.

Stone columns under superstructure compressive loads experience failure forms such as shear failure [1–3], bulging failure [4–9], and sliding failure [10], as illustrated in Figure 1. However, in soft soil, the common failure form of stone columns is bulging [7, 11–15]. When stone columns are constructed in very soft soils or within layered soils where the upper layer is very weak, they may not derive a significant bearing capacity because of the low lateral confinement leading to excessive bulging [13, 16].

* Corresponding author: qiyaowang@tom.com

http://dx.doi.org/10.28991/CEJ-2022-08-10-01

© 2022 by the authors. Licensee C.E.J, Tehran, Iran. This article is an open access article distributed under the terms and conditions of the Creative Commons Attribution (CC-BY) license (http://creativecommons.org/licenses/by/4.0/).

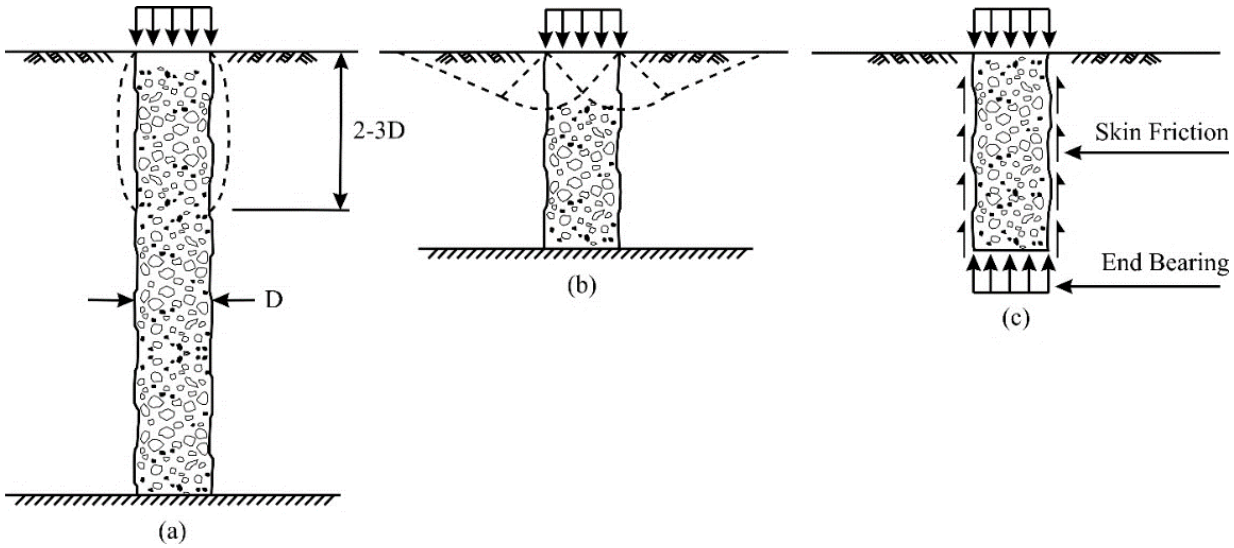

Figure 1. Failure mechanism of single stone column in homogenous soft soil [7]; (a) Long stone column with or without floating support: bulging failure, (b) Short column with rigid base: shear failure, (c) Short floating column: punching failure

The high bearing capacity of the ground is associated with the high bearing capacity of the stone column. Various strategies have been proposed to improve the stone columns' performance and the bearing capacity reaction in all weak soil types. For example, Sharma et al. [17] used layers of horizontal geogrid in the upper part of stone columns; Rao & Bhandari [18] used strong concrete parts and cement grout to improve lateral column bulging; Juran & Riccobono [19] recommended mixing the granular stone material with cement at the top of the columns. The bearing capacity of stone columns depends on the lateral confinement of columns offered by the surrounding soil [4, 20, 21]. Shallow soil with low lateral confinement may not support the columns' excessive bulging deformation [22].

Based on the failure modes of stone columns, several new concrete-stone columns have been developed. This concrete-stone column (CSC) has much higher bending and compressive (sometimes tensile) capacities than the stone column without reinforcing components [23]. The aims were to understand the capacity improvement of the concrete-stone columns by including the concrete solid parts on their top and comprehensive (CSC) behavior. Figure 2 shows a concrete-stone composite column, in which a pre-installed stone column is embedded in a solid concrete part [24]. The (CSC) can also be shaped by pouring concrete into the upper part of an ordinary stone column [23].

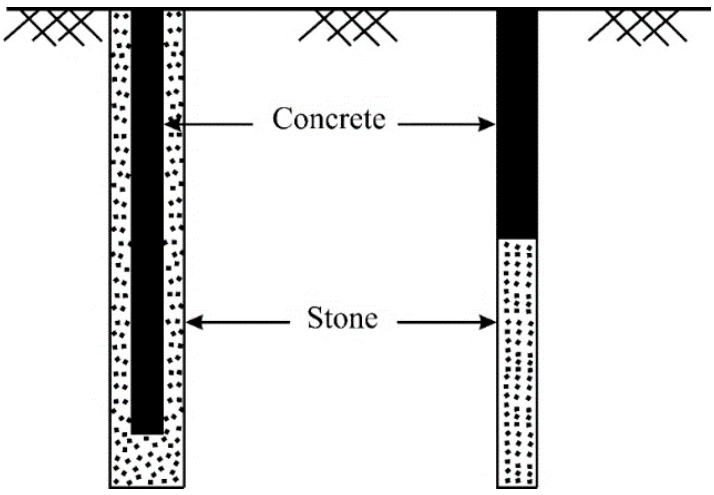

Figure 2. Concrete-stone column (composite form of the ordinary stone column and pile)

We assumed that the new model of (CSC) system has additional improvements for the stiffer core, similarly, the horizontal stress, bulging resistance, and stress ratio would all be affected. In this academic study, an experimental investigation is carried out on a single stone column properly installed in loess soil; the investigation included an ordinary stone column and four concrete-stone columns. The study focused on knowing the columns' behavior and the influence of concrete-stone columns on loess soil with various parameters. Loess soil was carefully adjusted according to the native state in the extracted site with the typical water contact and soil density. The paper describes the specific details of experimental work carried out and numerical analysis using the finite-element package. Figure 3 shows a flowchart of the research methodology.

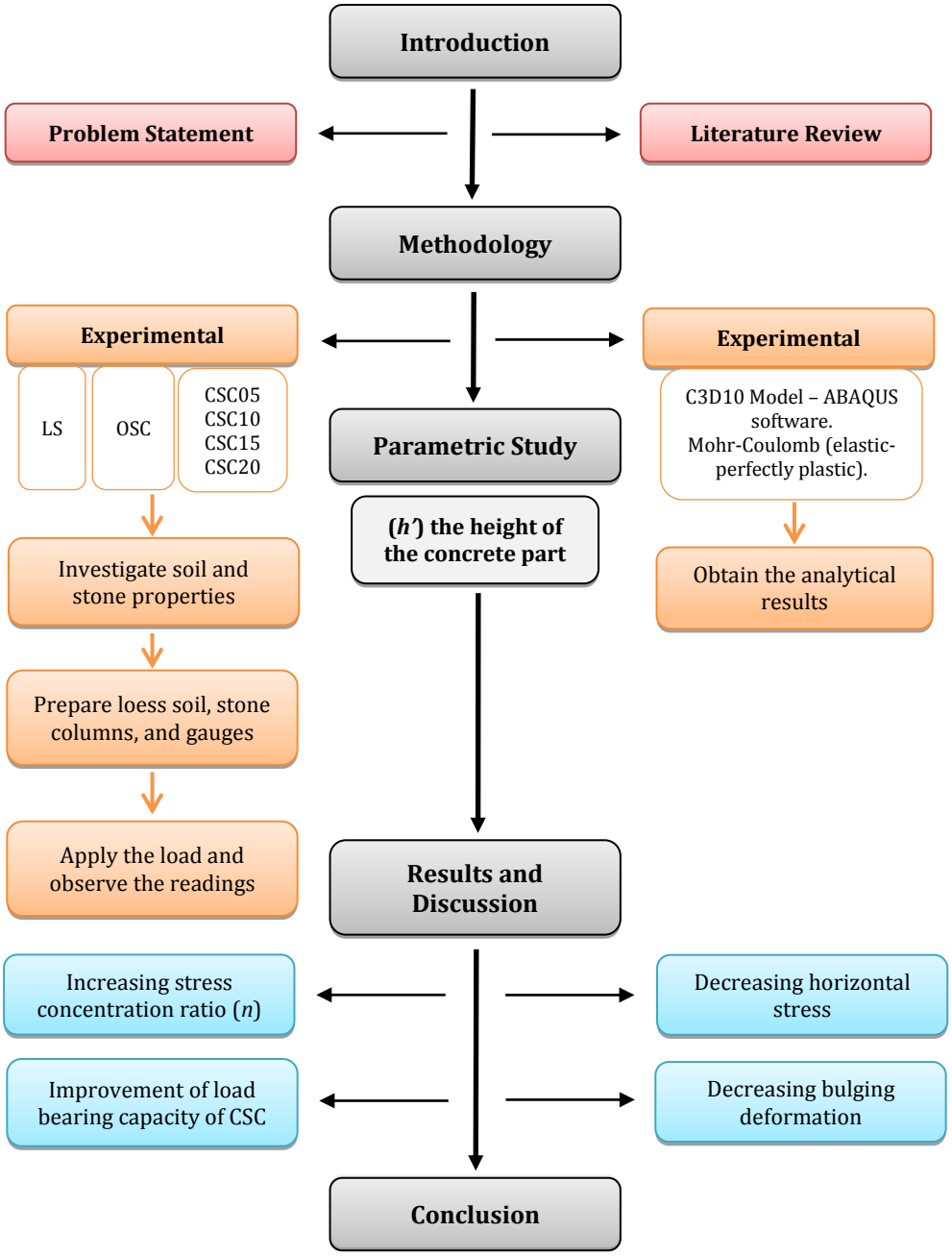

Figure 3. Research methodology flowchart

2. Experimental Programme

All the tests were carried out in a large fabricated steel box of 700 mm in plan and 800 mm in height, as shown in Figure 4. The diameter of model stone columns (100 mm) and the length (540 mm) were approximately in 1:7 scale, representing prototype stone columns of 700 mm diameter and 4000 mm length. The failure zone of a rigid pile expands downward over an approximate depth of two times its diameter [25]. This depth would be reduced due to the stone columns flexibility. Thus, a soil layer with 100 mm was lies under the stone columns. In some studies, it has been reported that the failure wedge in the foundation bed soil extends for a distance of 2–2.5 times the footing width away from the center (D) [26-28]. A circular plate with a diameter of 230 mm and a thickness of 25 mm was used as a loading plate in this study. The failure wedge does not intervene with the box's walls because the distance between the box's walls and the center of the footing is greater than 2.5D. To achieve the natural state of loess soil, the unit weight-control method was used to fill the box with loess soil; the loess soil was filled in the box in layers of 10 cm thickness and compacted with a steel hammer. A density test was taken for each layer to control the required density.

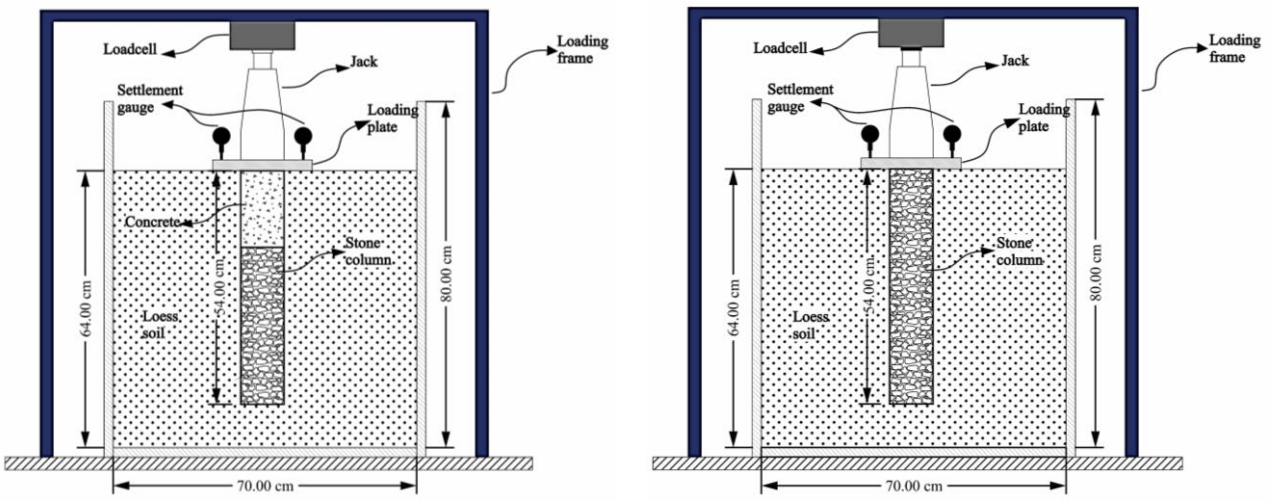

Figure 4. Test setup schematic diagram (a) OSC, and (b) CSC

The data-acquisition system, the loading frame, the loading plate, and the loading jack were all component of the loading system. The data-acquisition systems involved a DH3816 static-strain acquisition instrument, a computer, eleven earth pressure gauges, load cell, and a digital watch. Two displacement gauges were located on the loading plate to show the jack-loading displacement. A schematic diagram of an experimental setup is shown in Figure 5. The earth pressure gauges utilized were class DMTY with 500 kPa capacity and a 2.5 cm diameter for measuring the horizontal and vertical stresses along the stone column's length. The load cell used was of class DMHZ and had a capacity of 10 tons and 12 cm diameter for measuring the total force on the loading plate.

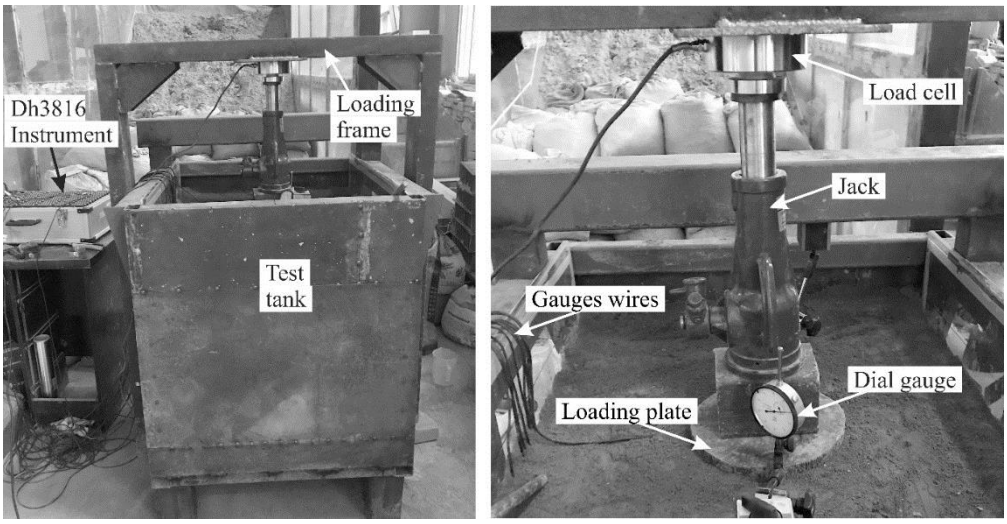

Figure 5. Illustrates the test tank and loading system; (a) test tank and loading frame (b) loading plate, jack, gauges, and load cell

All tests were performed based on a loading rate of 1 mm/minute till the full penetration with a displacement of 30 mm was achieved. Six tests were carried out in total, with some of them being repeated to ensure that the results were repetitive and consistent. The details of the test are summarized in Table 1.

Table 1. Summary of the experimental program

Test. No	Test name	Test description
1	LS	Only loess soil
2	OSC	Ordinary stone column
3	CSC05	Concrete-stone column with 5 cm concrete part
4	CSC10	Concrete-stone column with 10 cm concrete part
5	CSC15	Concrete-stone column with 15 cm concrete part
6	CSC20	Concrete-stone column with 20 cm concrete part

2.1. Material Properties

2.1.1. Loess Soil

Loess soil layers were prepared in the laboratory using locally available soil previously collected from construction sites in Xi'an city, China. A 1.0 mm sieve was used to remove coarse granular and plant remains from the soil. The granular size distribution was determined through laser particle analysis on the Bettersize2000 machine; Figure 6 illustrates the particle size distribution curve. Using the IS classification system, the soil sample is categorized as MI, and the other characteristics of loess soil are listed in Table 2.

Table 2. Properties of loess soil

Parameter	Value
Specific gravity	2.65
Liquid limit (%)	33.5
Plastic limit (%)	20
Plasticity index (%)	13.6
Coefficient of permeability	6.77×10^{-10} m/s
Maximum dry unit weight	18.8 kN/m
Optimum moisture content (%)	16
Bulk unit weight at 18% water content	21.2 kN/m^3
IS classification symbol	MI

2.1.2. Stones

Crushed stone aggregates typically ranging from 12 to 3 mm were used to form the stone column. Figure 6 shows the granule size distribution for stone columns. D_{10}, D_{50}, and D_{90} are 3.2, 6.5, and 10.5 mm, respectively. According to the IS classification, the stone material mixture is classified as poorly graded gravel or GP. The maximum granular size of the stone material used is 1/8 of the column's diameter (12 mm); this ratio is marginally smaller than Nayak's guidelines [29, 30]. A direct shear test was carried out to estimate the stone materials' internal friction angle, and the relationship ($\Psi = \phi - 30$) was used to calculate the dilation angles. Modulus of elasticity and the Poisson's ratio used are typical values suggested by Bowles [31]. Table 3 summarizes the properties of the stone column material.

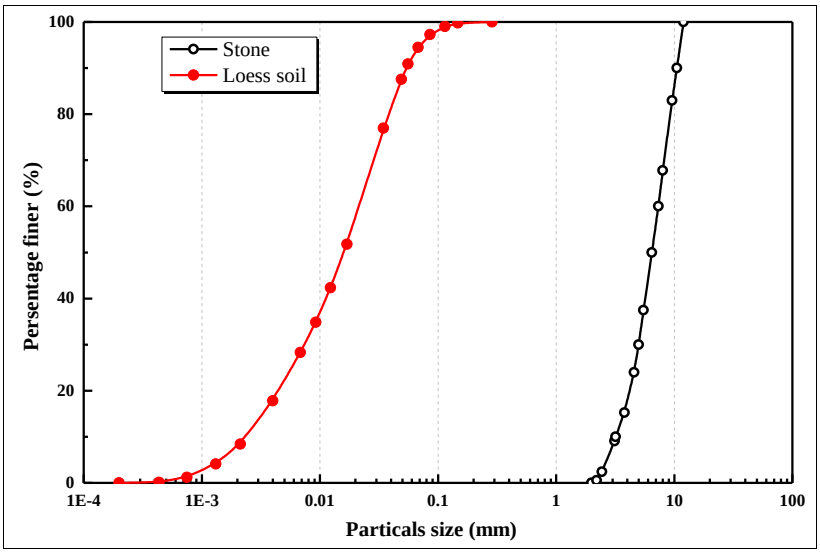

Figure 6. Particle size distribution for stone column and loess soil materials

Table 3. Properties of stone column material

Parameter	Value
Specific gravity	2.7
Maximum dry unit weight	16.7
Minimum dry unit weight	14.5
Bulk unit weight for test at 70% relative density	16
Internal friction angle at 70% relative density	45
Uniformity coefficient *Cu*	2.28
Curvature coefficient Cc	1.07
IS classification symbol	GP

2.2. Preparation of Layered Loess Soil Stratum

The unit weight control method was adopted to prepare the soil bed in all the tests. The primary water content of loess soil was calculated to evaluate the water required to reach 18%, which provides 21.2 bulk unit weight. Six equal layers of 100 mm thickness with a similar unit weight were used to fill the box in each test. A bulk unit weight of 21.2 kN/m^3 was considered to estimate the required soil in each layer. A special steel tamper 150 mm in diameter and 10 kg in mass was utilized to compact each layer to achieve the required thickness. They were compacted to a height of 540 mm, and the final soil layer was levelled to ensure a suitable, cavity-free surface. All experimental tests were carried out using the same fabrication method. During soil preparation, the water content percentage variation was below 1%. During filling the box, bulk unit weight was measured for each layer to ensure that the soil unit weight was kept around 20 kN/m^3.

During filling the soil into the box, earth pressure gauges were placed along the column side to estimate the horizontal stress caused by bulging deformation. Further, earth pressure gauges were provided below the load plate to measure the stress ratio change of soil around the column under the load's action. It should be mentioned that the earth pressure gauge has both positive and negative sides. When they are placed, it should be noted which side faces the applied stress.

2.3. Construction of Stone Column

All stone columns were constructed in the center of the test box using the replacement method. The stone columns were constructed using an open-ended stainless-steel pipe without any seam, the thickness of the pipe is 2 mm, and its inner diameter is 100 mm. The steel pipe's external surface was painted with oil to reduce the friction while pulling out the pipe. The pipe was placed at the center mark then loess soil beds were formed in layers around it. The stones were weighted and carefully placed into the pipe; they were compacted using a 16 mm diameter rod to achieve a uniform density of 16 kN/m^3. This process was replicated till the entire stone column was created. Four parts of normal-weight concrete with a density of 23.3 kN/m^3 and 24 MPa compressive strength were used to create the concrete-stone columns on the column's top. They were formed in a cylindrical shape with 100 mm diameter and different lengths of 50, 100, 150, 200 mm.

2.4. Test Procedure

The whole experimental process consists of three stages. The first stage is preparing the loess soil bed and installing the stone column and the pressure gauges. The second stage comprises the load application on the tributary area. The third stage includes, the load value and the correlating settlement were gauged using load cells and settlement dial gauges. The measurements were conducted to estimate the entire tributary area's vertical stress compared to the settlement characteristics.

The stone column and the surrounding soil's stress-settlement behavior were considered by applying the jack's vertical load supported by a loading frame. After completing the soil filling and the column construction and calibration of the static-strain acquisition instrument and earth pressure gauges, the tributary area was loaded. The reading of load cell and earth pressure gauges was taken through data-acquisition systems connected to the computer. A constant loading rate of 1 mm/minute was applied [32, 33]. The loading was kept steady for half an hour until the settlement reached 30 mm. While filling the steel pipe with stones, a 0.8 mm sheet of aluminum foil was placed on the side of the pipe. Since the aluminum foil sheet material has the ability to be deformed easily, it was employed to measure the amount of bulging deformation that occurs in the column after the loading process. After completing the experiment, the stones were removed very carefully not to affect the aluminum foil sheet. Then it was taken out, and the amount of deformation that had occurred to the sheet was measured.

2.5. Models Used for Numerical Study

3D finite-element models of the exact size as the laboratory model tests were developed and analyzed with ABAQUS software, see Figure 7. The numerical model, constraints, parametric studies, and material properties are tabled. The Mohr-Coulomb elastic-perfectly plastic failure criterion has been used for loess soil and stone [34]. The concrete part was considered elastic material in this analysis, given that the concrete failure point is much further than the failure point of the stone column and the surrounding soil. The gravity load has been considered to produce the initial stress conditions.

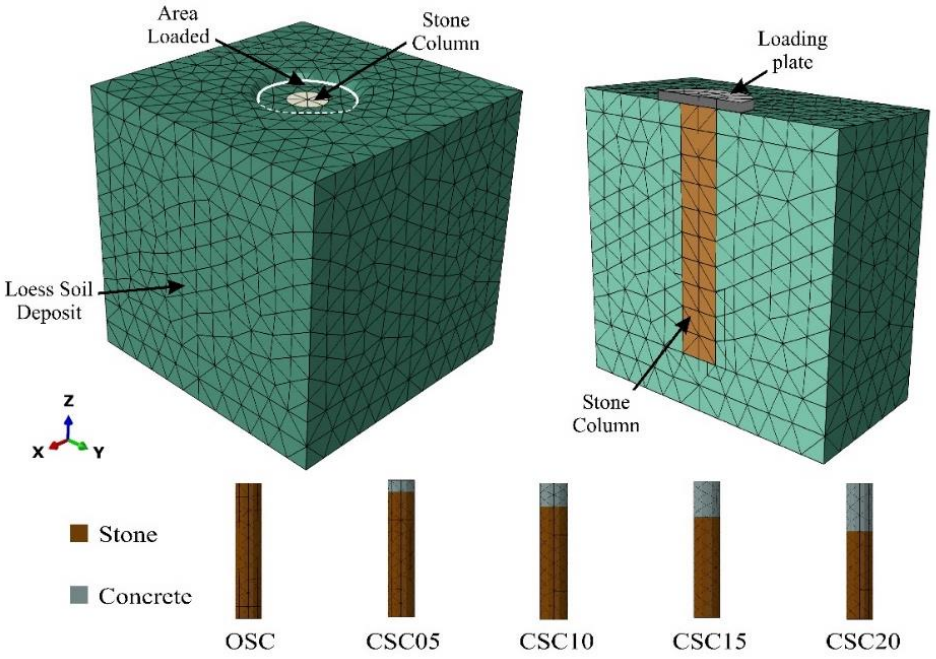

Figure 7. 3D Mesh geometry of the FE model, OSC and CSCs models

Table 4 epitomizes the parameters used for numerical analysis. Young's modulus, internal friction angle, and loess soil and stones' cohesion have been determined from the relevant laboratory tests. The Poisson's ratio of loess soil and stone were taken from [31], and the dilation angle values have been found from the relationship $\Psi=\phi-30^{\circ}$. C3D10 (10-node quadratic tetrahedron) model has been used to discretize the stone column and the surrounding soil. The whole model meshed with an approximate element size of 0.06, as shown in Figure 7.

The stone columns were adopted in a tight overlapping pattern with the surrounding soil [35]. On all interfaces, the tie constraints were employed (i.e., full fixation at the interfaces). The constraints at the interfaces of soil, columns, and concrete part are represented as tie constraints with perfect bonding [36, 37]. All the nodes along the periphery side of the loess soil bed were considered a roller, and all the nodes in the bottom face of the loess soil bed were restrained using fixed support. The upper side is free to move in any direction.

Table 4. Input parameters employed in the finite element analysis

Parameters	Properties		
	Loess soil	Stone	Concrete
Modulus of elasticity (MPa)	3.0	30	200
Poisson's ratio (μ)	0.2	0.22	0.18
Shear strength (kPa)	30	0	-
Internal friction angle (ϕ)	0	33	-
Dilation angle (Ψ)	0.1	3.0	-
γ_{bulk} (kN/m^3)	1.96	1.65	-

3. Results and Discussions

3.1. Stress-Settlement Behavior

Figure 8 shows the bearing capacity (stress) of unreinforced soil and soil reinforced with OSC. The reinforced soil illustrates the enhancement of soil when the OSC was embedded. The figure also shows that the bearing capacity of loess soil increased by 12.6% in 30 mm settlement. Moreover, the bearing capacity increment is even higher when using concrete-stone columns. As a matter of fact, CSCs prevent the bulging deformation near the ground surface, and increase the stiffness of the improved soil area; therefore, soil bearing capacity increases. The soil stress-settlement curves of reinforced soil enhancement by the concrete-stone column are shown in Figure 9. As reveal, the bearing capacity improved as the concrete part increased in length. The concrete part with 50, 100, 150, 200 mm length represents 9, 18.5, 27.7, 37% of the stone column's total length, respectively. According to Table 5, the bearing capacity increases to 32.6, 36, 38.7, and 48.3 if a concrete part is used with a length of 50 mm (CSC05), 100 mm (CSC10), 150 mm (CSC15), and 200 mm (CSC20), respectively.

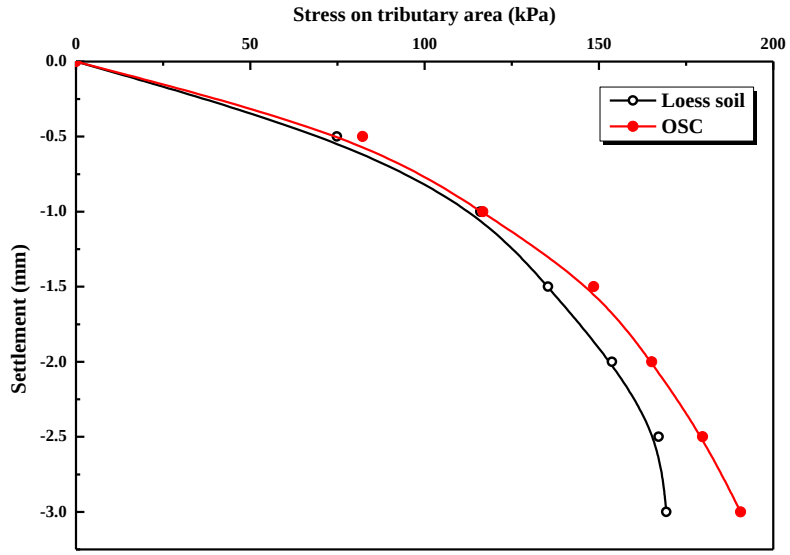

Figure 8. Stress-settlement variation of unreinforced loess soil and reinforced loess soil with ordinary stone columns

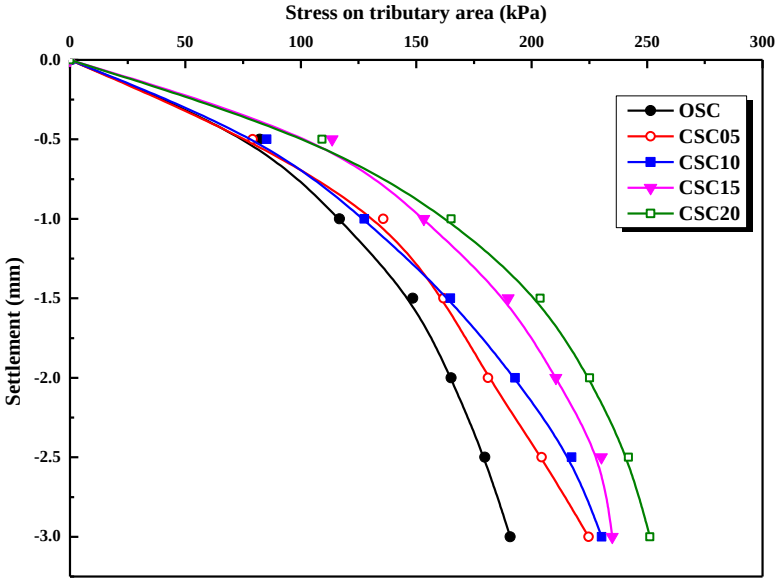

Figure 9. Stress-settlement variation of unreinforced soil and reinforced soil with OSC

Table 5. Percentage of increased bearing capacity and the ratio of the concrete part length

Test	Increased bearing capacity (%)	Ratio of the concrete part length to the total length (%)
Loess Soil	-	-
OSC	12.6	-
CSC05 (*h'/l=9*)	32.6	9.0
CSC10 (h'/l=18.5)	36	18.5
CSC15 (*h'/l=28*)	38.7	27.7
CSC20 (*h'/l=37*)	48.3	37

Figure 9 shows that the concrete part provides greater bearing capacity and stiffness. In addition, under loading the rigid part moves down where the confinement stress is higher leads to reduce the lateral bulging of stone column. Moreover, by increasing the concrete part length, the bearing capacity of CSCs and the surrounding soil increases compared with that of OSC. For a vertical applied stress, the observed settlement is less when the *h'/l* ratio is increased; The higher the *h'/l* ratio is, the lesser the settlement.

The results obtained through FEM analyses show almost a similar trend as observed in experiments; they are compared in Figures 10 and 11. The stress-settlement response for OSC and CSCs using Mohr-Coulomb models for

loess soil and concrete-stone columns was compared with the corresponding experimental curves. The comparison is extremely valid, and the maximum difference in stress is 3.1%, as shown in Table 6 for a given settlement. Table 6 also shows the stresses for 30 mm settlement.

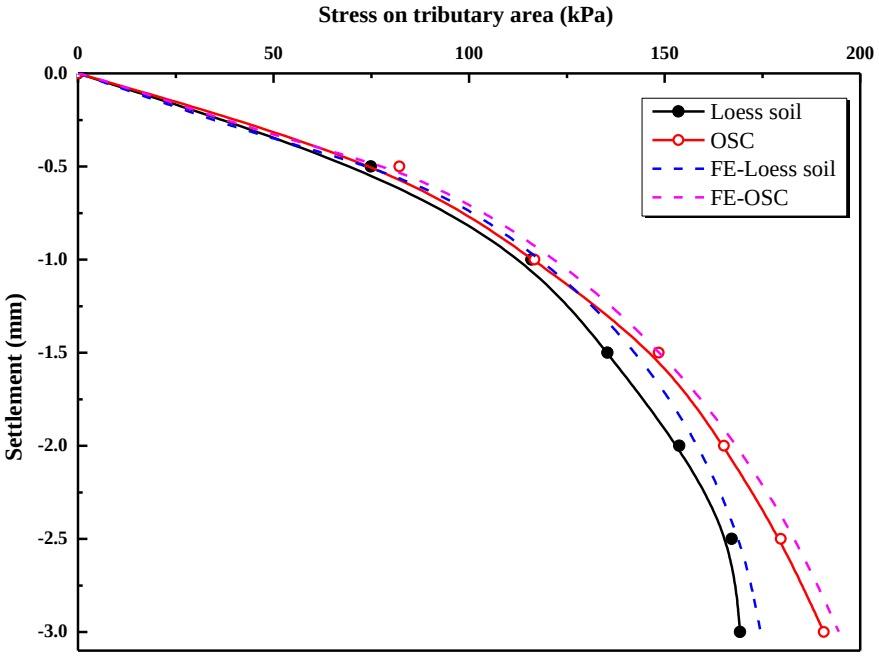

Figure 10. Stress-settlement variation of unreinforced soil and reinforced soil with OSC, experimental and numerical comparison

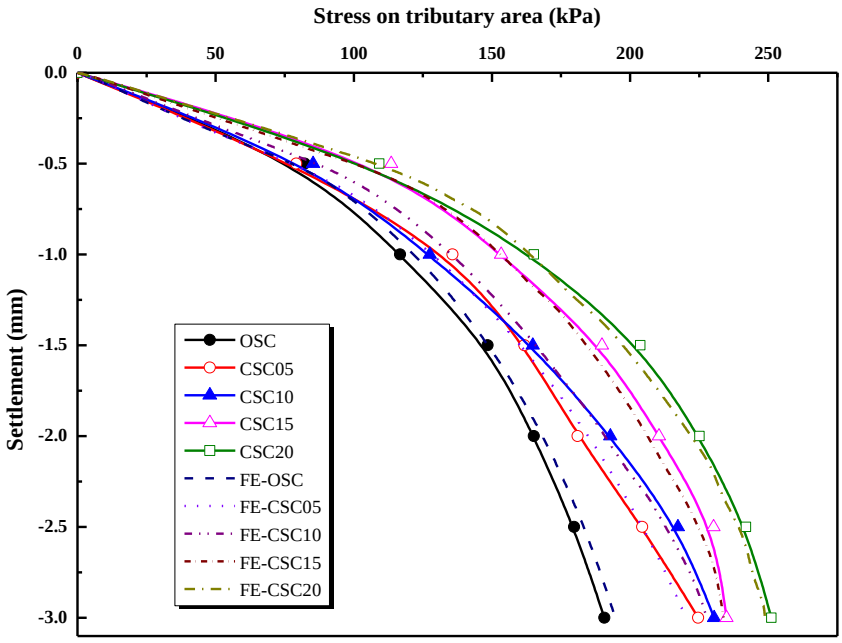

Figure 11. Effect of concrete-stone column on the capacity of tributary area, experimental and numerical comparison

Table 6. Load-bearing capacity of loess soil bed reinforced by stone column at 30 mm settlement

Model type	Exp. (kPa)	FEM (kPa)	The difference in Stress (%)
Loess soil	169	175	3.1
OSC	191	195	2.0
CSC05 (*h'/l=9*)	225	220	2.0
CSC10 (*h'/l=18.5*)	230	228	1.1
CSC15 (*h'/l=28*)	235	234	0.5
CSC20 (*h'/l=37*)	251	249	1.0

3.2. Improved Load Ratio

The test results were compared for a better understanding of the stone columns' efficiency. Figure 12 shows the load ratio-settlement variation for ordinary and concrete-stone columns. As indicated, the LR varies in the range of 1.10 - 1.60 for ordinary stone columns and concrete-stone columns having different (*h'/l*) ratios. The OSC shows the minimum LR while CSCs shows the maximum LR, moreover, CSCs have the largest (*h'*) displays the highest value of LR. This behavior is due to that, the concrete part increases the soil stiffness near the surface and precludes bulging from taking place. Figure 12 also presents that the LR value increases with increasing the loading up to a penetration ratio of about 20%, then slightly decreasing until reaching 33.3% penetration. This reduction is related to the repositioning of the stone particles due to overloading. The value of LR increases up to a settlement of about 15 mm, beyond it keeps almost constant.

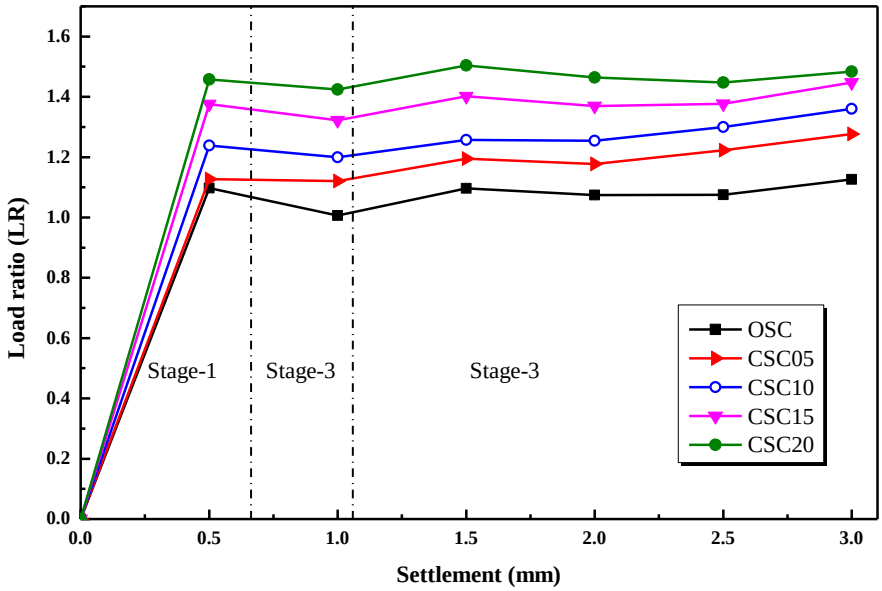

Figure 12. Load ratio variation versus settlement for OSC and CSCs

Referring to the ratio of the settlement value (*S*) to the concrete-column length ratio (*h'/l*), the settlement ratio is (*S/(h'/l)*). Figure 13 shows that the LR values are a little similar to the results in Figure 12, except that the settlement ratio (*S/(h'/l)*) is different from one model to another. For example, in model CSC05, LR continues to a value more than 30%, while it stands at the smallest value of 8% in CSC20. Settlement ratio is an effective indicator of the column compression value before it rich its full capacity. The model CSC20 tend to behave as a solid concrete pile; therefore, settlement ratio assists to indicate the significate (*h'/l*) ratio that does not lead to the depletion the characteristic of the stone column.

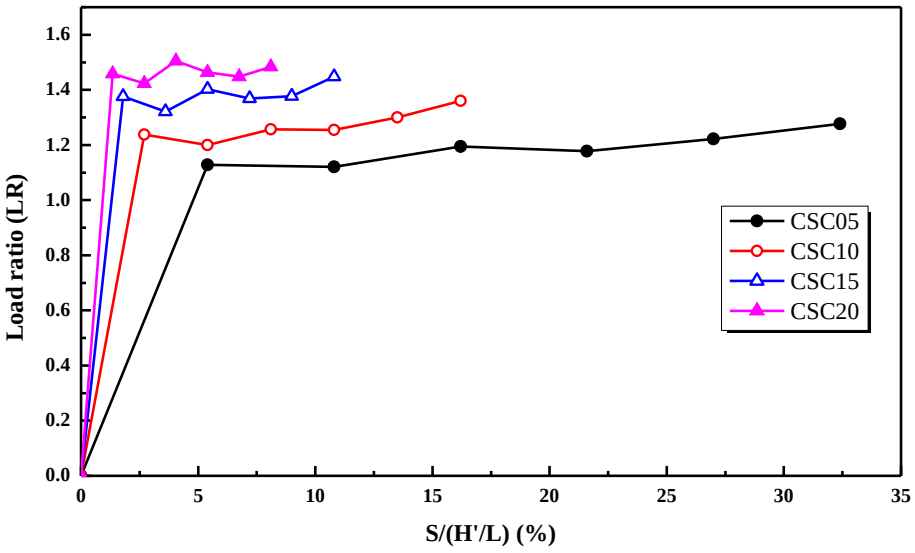

Figure 13. The load ratio affected by the concrete part length (h')

3.3. Stress Concentration Ratio *(n)*

The ratio of stone column stress to the surrounding soil stress is defined as the stress concentration ratio. Stress concentration occurs in the stone column as the soil is loaded, and as a result, a decrease in stress occurs in the surrounding loess soil. The stresses implemented on the stone columns are greater than that on the surrounding loess soil because it is more flexible than stone columns. Fattah et al. [30], Ambily & Gandhi [36], and Ghazavi & Afshar [38] estimated stress values on both the surrounding soil and stone columns to analyze the stress concentration ratio within stone columns. A prominent standard for the efficiency of stone columns is the load intensity on the stone columns, and it has been applied in their design. The stone column's load ratio is greater than that in the surrounding soil due to the stiffer stone columns, which increases the stress concentration in the stone column.

The stress concentration ratio (*n*) goes through three phases, as shown in Figure 14. The first phase is the phase where the stone column withstands all the pressure load itself. Therefore, the line's gradient in the first phase is slightly steeper than the second and third phases. The mechanical interlocking between grains in OSC increases (*n*) linearly up to almost 15.8%, then it keeps constant till reaching the highest penetration. While in CSCs, a linear increasing in (*n*) occurs due to the mechanical interlocking and in-place densification of stone column material, the maximum (*n*) reaches 30.5, 54.6, 70.7, 100 percent. The fraction between the concrete part and surrounding loess soil played a significant role in increasing (*n*). The second phase indicated a reduction in the stress concentration ratio, the rate of reduction varies according to the height of the concrete part. The overloading on CSCs reduces (*n*) at a penetration higher than 2.5%. This overloading is associated with high axial stress on concrete parts, which compress stone column grains toward the surrounding loess soil. This behavior induces a gradual transfer of the load to the loess soil; therefore, (*n*) decreases consequently. For the third phase, the stresses are distributed equally between the column and the surrounding soil.

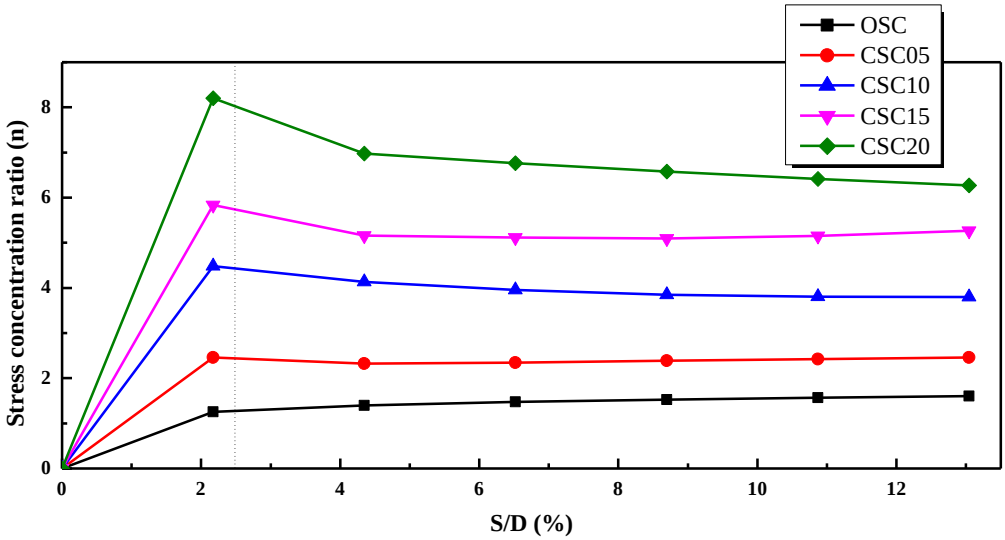

Figure 14. Stress concentration ratio versus the penetration ratio

Phase-1 lay between 0 - 5 cm, while phase-2 lay between 5 - 10 cm; after the 10 cm settlement, phase-3 was shown. The concrete-stone column's behavior is similar to the encased stone column's behavior, as discussed in the study conducted by Ghazavi & Nazari Afshar (2013) [38].

The minimum stress concentration ratio of 1.6 was noticed in the OSC model, while the maximum value for the CSC20 model was 6.3 at maximum penetration. This indicates that the (*n*) value increases as well as the column stiffness by increasing the length of the concrete part. Table 7 presents the (*n*) maximum values reached; and the (*n*) value reduction in OSC and CSCs.

Table 7. The maximum stress concentration ratio at 2.5% penetration and stress reduction of CSCs

Tests	(*n*)	Max. (*n*) at 2.5% penetration	Value of reduction %
OSC	1.6	1.3	-
CSC05	2.5	2.5	0
CSC10	3.8	4.48	18
CSC15	5.3	5.8	10
CSC20	6.3	8.2	30

3.4. Bulging of Stone Column

Bulge deformation occurs close to the column's top, where the confining pressure is the lowest as reported in previous studies. The concrete part was utilized to overcome this deformation near the ground surface, leading to increased column bearing capacity.

The magnitude of bulging was measured following column failure using an aluminum foil sheet, as previously discussed. Figure 15 illustrates that, for CSCs, the maximum bulging occurred directly at a depth of about 60 mm (≈0.5d) below the concrete part; a similar bulging depth of 0.5d was also reported by Ambily & Gandhi [36]. Likewise, the maximum bulging occurred at a depth of 110 mm (≈1d) in the OSC; the value of bulging depth ranges 1.0d – 2.5d was reported by Lee et al. [39]. When CSC05 enhances the loess soil bed, a 30% reduction in maximum bulging deformation is observed, while OSC showed very high stress near the ground surface, which caused a high bulging. Moreover, a significant stress reduction occurs on top of the stone column when concrete parts are placed over it; thus, a low bulging is recorded. The results indicate that, the bulging deformation decreases with increasing the length of the concrete part. The maximum bulging variation and bulging depth for different concrete part lengths are presented in Table 8.

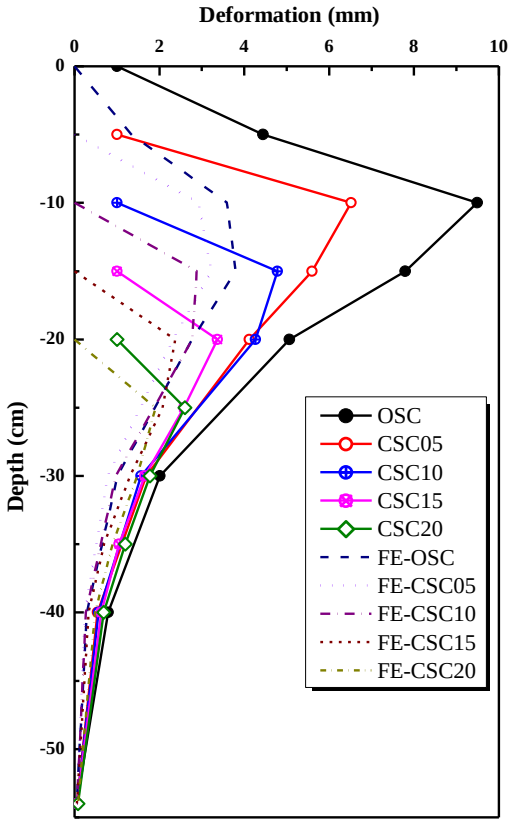

Figure 15. Experimental and numerical lateral deformation along the length of stone column for OSC and CSCs

Table 8. The maximum bulging and the bulging redaction ratio for all stone column models

Test	Concrete part length (mm)	Max. bulging (mm)	Depth of bulging (mm)	Bulging redaction compared with OSC %
OSC	-	9.5	110	-
CSC05	50	6.8	110 + 60 =170	30
CSC10	100	5.0	170 + 60 =230	47
CSC15	150	3.4	230 + 60 =290	64
CSC20	200	2.6	290 + 60 =450	73

3.5. Horizontal Stress

Several previous studies estimated the value of horizontal stresses using lateral earth pressure coefficient K, as an empirical relationship suggested by Brooker & Ireland [40]: $K = 0.95 - sin\,\phi$. This K coefficient is utilized in the numerical analysis to determine the horizontal stresses. In this study, the experimental method was considered to estimate the horizontal stresses. On the stone column's side, numbers of earth pressure gauges were placed to calculate the horizontal stress generated by the vertical load on the column. The pressure gauge's top face was facing the soil to measure the magnitude of stress reaction caused by the stone column's bulging deformation.

Figure 16 presents the horizontal stress in the soil caused by the stone column's compressive bulging deformation. The horizontal stress is related to the amount of bulging deformation in the column. The horizontal stress is equal to the vertical stress on the soil ground surface at maximum settlement. Moreover, the horizontal stress increases as the depth increase until reaching the maximum value then decreases as the depth increases to the bottom of the column, but it did not reach zero.

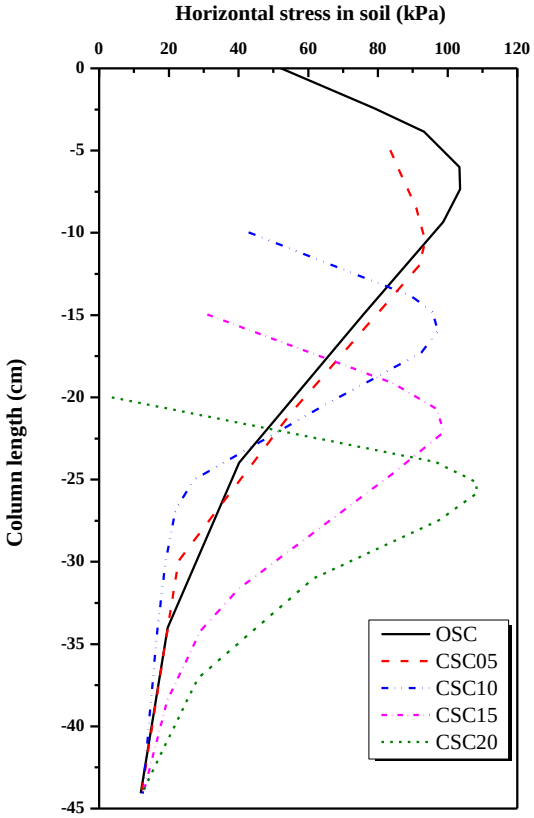

Figure 16. Horizontal stress in soil along with column length for OSC and CSCs

The highest value of horizontal stress in the ordinary stone column (OSC) was 100 kPa at a depth of 60 mm from the soil ground surface. The first model of the concrete-stone column (CSC05) reported a 10% reduction in horizontal stress; horizontal stress occurred at a depth of 60 mm underneath the concrete part. The horizontal stresses showed a slight increase in the second and third models (CSC10 and CSC15). The fourth model (CSC20) displayed a higher amount of horizontal stress, even higher than that of the OSC; this is because the fourth model - with a concrete part of 200 mm length - has become a short column and susceptible to failure due to shear failure, and short column tend to fail under shear as mentioned in Sivakumar's study [41]. This indicates that shear stress was the cause of the increased horizontal stress in the fourth model, and this increase was not due to the bulging deformation.

It should be noted that as long as the ratio of the concrete length to the total column length does not exceed one-third, shear failure will not occur. In addition, the highest value of horizontal stress in all models occurred at 60 mm depth. Meaning, the critical depth of maximum horizontal stress is 0.6d.

4. Conclusions

In this paper, experimental studies were performed on ordinary stone columns and concrete-stone columns. Four different lengths (50, 100, 150, and 200 mm) of concrete parts were used. The ordinary stone column was compounded with a concrete part. According to the observation of experimental tests and parametric study through FEM analysis, the following conclusions are drawn:

- Using either ordinary stone columns or composite-stone columns improved the ultimate bearing capacity. The use of concrete part over pre-installed stone columns enhanced the stone columns' performance. The concrete part with a length of 200 mm has a significant influence on soil improvement compared to the concrete part with a 5.0 mm length;
- The 5.0 mm concrete part length application increases the bearing capacity by 32.6% compared with unenhanced soil. A stone column with a solid concrete part increases the stiffness of the enhanced soil area. The lengthier the concrete part is, the higher is the load-carrying capacity;

- The (*h'/l*) ratio is a critical parameter that may indicate the capacity of the stone column. The stone column's capacity increases with an increasing (*h'/l*) ratio, which in turn leads to a reduction in the settlement;
- Using ordinary stone columns is more economical than using concrete-stone columns. However, CSC provides more enhancement to the weak loess soil, resulting in an economic foundation for buildings. Moreover, concrete material is available and inexpensive, so CSCs consider it an acceptable treatment method for weak soil improvement;
- The CSCs' load ratio reaches the highest values at 20% penetration ratio, then consequently decreases. Moreover, the LR reduction is due to the repositioning of the stone particles under vertical overloading. The maximum LR was recorded in the concrete-stone column with a 200 mm concrete part length (CSC20);
- It has been noticed that a penetration ratio of approximately 33.3% occurred at the highest increasing rate of LR. Beyond that, the LR value is nearly constant. Besides, it is noted that, by using concrete part along with the stone columns (CSCs), the value of the load ratio increases because of an increase in the composite foundation stiffness;
- The use of the concrete part enhances the stress concentration ratio (*n*) and bearing capacity of stone columns. Moreover, the concrete part reduces bulging, thereby increasing the bearing capacity of stone columns;
- It has been proven that an ordinary stone column (OSC) has an excessive bulge (110 mm) caused by a lack of lateral confinement pressure. On the contrary, the concrete-stone columns (CSCs) showed good behavior, namely a much reduction in bulging. 30% bulging redaction in the model (CSC05), (CSC20) indicated a higher reduction of about 60% compared with OSC;
- The OSC displayed the maximum value of horizontal stress, about 100 kPa. CSC decreases the horizontal stress as they increase the stiffness of the surrounding soil and the column. The stresses value in (CSC05), (CSC10), and (CSC15) illustrated no significant reduction. But, in the model (CSC20), the stone column part is considered a short column; therefore, it is subjected to shear failure, so the horizontal stress is relatively higher.

5. Declarations

5.1. Author Contributions

Conceptualization, M.A.S. and Q.W.; methodology, M.A.S.; software, M.A.S.; validation, M.A.S. and J.H.; formal analysis, M.A.S. and J.H.; investigation, M.A.S.; resources, M.A.S. and J.H.; data curation, M.A.S. and J.H.; writing—original draft preparation, M.A.S.; writing—review and editing, M.A.S. and J.H.; visualization, M.A.S. and Q.W.; supervision, Q.W.; All authors have read and agreed to the published version of the manuscript.

5.2. Data Availability Statement

The data presented in this study are available in the article.

5.3. Funding

The study was approved by the National Natural Science Foundation of China (Grant nos. 51379015 and 51579013) and the Fundamental Research Funds for the Central Universities, CHD (Grant no. 300102289303).

5.4. Acknowledgements

I would like to pay my sincere gratitude to my supervisor Dr. Qiyao Wang, Professor of Civil Engineering Department, for providing generous guidance and modest discussion time. I acknowledge the kindness and infinite patience shown in all matters.

5.5. Conflicts of Interest

The authors declare no conflict of interest.

6. References

[1] Madhav, M. R., & Vitkar, P. P. (1978). Strip Footing on Weak Clay Stabilized with a Granular Trench or Pile. Canadian Geotechnical Journal, 15(4), 605–609. doi:10.1139/t78-066.

[2] Wong, H. Y. (1975). Vibroflotation-its effect on weak cohesive soils. Civil Engineering (London), 82, 44-76.

[3] Barksdale, R. D., & Bachus, R. C. (1983). Design and construction of stone columns. Report No. FHWA/RD-83/026;SCEGIT-83-104, Office of Engineering & Highway Operations Research and Development, Federal Highway Administration, Washington, United States.

[4] Hughes, J. M. O., Withers, N. J., & Greenwood, D. A. (1975). A Field Trial of the Reinforcing Effect of a Stone Column in Soil. Geotechnique, 25(1), 31–44. doi:10.1680/geot.1975.25.1.31.

[5] Greenwood, D. A. (1970). Mechanical improvement of soils below ground surface. Institution of Civil Engineers, London, United Kingdom.

[6] Vesić, A. S. (1972). Expansion of Cavities in Infinite Soil Mass. Journal of the Soil Mechanics and Foundations Division, 98(3), 265–290. doi:10.1061/jsfeaq.0001740.

[7] Hughes, J. M. O., & Withers, N. J. (1974). Reinforcing of soft cohesive soils with stone columns. International Journal of Rock Mechanics and Mining Sciences & Geomechanics Abstracts, 11(11), A234. doi:10.1016/0148-9062(74)90643-3.

[8] Datye, K. R., & Nagaraju, S. S. (1975). Installation and testing of rammed stone columns. Proceedings of IGS specialty session, 5th Asian Regional Conference on Soil Mechanic and Foundation Engineering, 101-104, Bangalor, India.

[9] Madhav, M. R., Iyengar, N. G. R., Vitkar, R. P., & Nandia, A. (1979). Increased bearing capacity and reduced settlements due to inclusions in soil. Proceedings of International Conference on Soil Reinforcement, Reinforced and other Techniques, 239-333, 20-22 March, 1979, Paris, France.

[10] Sakr, M., El-Sawwaf, M., Azzam, W., & El-Disouky, E. (2021). Improvement of shear strength and compressibility of soft clay stabilized with lime columns. Innovative Infrastructure Solutions, 6(3), 1-20. doi:10.1007/s41062-021-00509-w.

[11] Hughes, J. M. O., Withers, N. J., & Greenwood, D. A. (1975). A field trial of the reinforcing effect of a stone column in soil. Geotechnique, 25(1), 31-44. doi:10.1680/gtbdc.00247.0003.

[12] Ekeleme, A. C., Ekwueme, B. N., & Agunwamba, J. C. (2021). Modeling Contaminant Transport of Nitrate in Soil Column. Emerging Science Journal, 5(4), 471-485. doi:10.28991/esj-2021-01290.

[13] Shivashankar, R., Babu, M. R. D., Nayak, S., & Rajathkumar, V. (2011). Experimental Studies on Behaviour of Stone Columns in Layered Soils. Geotechnical and Geological Engineering, 29(5), 749–757. doi:10.1007/s10706-011-9414-0.

[14] Das, P., & Pal, S. K. (2013). A study of the behavior of stone column in local soft and loose layered soil. Electronic Journal of Geotechnical Engineering, 18, 1777–1786.

[15] Han, J. (2015). Recent research and development of ground column technologies. Proceedings of the Institution of Civil Engineers: Ground Improvement, 168(4), 246–264. doi:10.1680/grim.13.00016.

[16] Dheerendra Babu, M. R., Nayak, S., & Shivashankar, R. (2013). A Critical Review of Construction, Analysis and Behaviour of Stone Columns. Geotechnical and Geological Engineering, 31(1), 1–22. doi:10.1007/s10706-012-9555-9.

[17] Sharma, R. S., Kumar, B. R. P., & Nagendra, G. (2004). Compressive load response of granular piles reinforced with geogrids. Canadian Geotechnical Journal, 41(1), 187–192. doi:10.1139/t03-075.

[18] Rao, B. G., & Bhandari, R. K. (1980, May). Skirting—a new concept in design of heavy storage tank foundation. Proceedings of the 6th South-East Conference on soil Engineering, 283-300, 23 May, 1980, Taipei, Taiwan.

[19] Juran, I., & Riccobono, O. (1991). Reinforcing soft soils with artificially cemented compacted-sand columns. Journal of geotechnical engineering, 117(7), 1042-1060. doi:10.1061/(ASCE)0733-9410(1991)117:7(1042).

[20] Black, J. A., Sivakumar, V., Madhav, M. R., & Hamill, G. A. (2007). Reinforced Stone Columns in Weak Deposits: Laboratory Model Study. Journal of Geotechnical and Geoenvironmental Engineering, 133(9), 1154–1161. doi:10.1061/(asce)1090-0241(2007)133:9(1154).

[21] Mckenna, J. M., Eyre, W. A., & Wolstenholme, D. R. (1976). Performance of an embankment supported by stone columns in soft ground. Ground Treatment by Deep Compaction, 25(1), 52–59. doi:10.1680/gtbdc.00247.0005.

[22] Moseley, M. P., & Kirsch, K. (2004). Ground improvement. CRC Press, Boca Raton, United States. doi:10.2472/jsms.42.1023.

[23] Zheng, G., Liu, S., & Chen, R. (2009). State of Advancement of Column-Type Reinforcement Element and Its Application in China. Advances in Ground Improvement. doi:10.1061/41025(338)2.

[24] Chen, J. S., Tang, T. Z., Zhao, W. B., & Yu, J. (2007). Field tests on composite foundation with concrete-cored sand-gravel piles. Yantu Gongcheng Xuebao/Chinese Journal of Geotechnical Engineering, 29(7), 957–962.

[25] Meyerhof, G. G., & Sastry, V. V. R. N. (1978). Bearing Capacity of Piles in Layered Soils - 2. Sand Overlying Clay. Canadian Geotechnical Journal, 15(2), 183–189. doi:10.1139/t78-018.

[26] Selig, E. T., & McKee, K. E. (1961). Static and Dynamic Behavior of Small Footings. Journal of the Soil Mechanics and Foundations Division, 87(6), 29–45. doi:10.1061/jsfeaq.0000378.

[27] Latha, G. M., & Somwanshi, A. (2009). Bearing capacity of square footings on geosynthetic reinforced sand. Geotextiles and Geomembranes, 27(4), 281–294. doi:10.1016/j.geotexmem.2009.02.001.

[28] Verghese Chummar, A. (1972). Bearing Capacity Theory from Experimental Results. Journal of the Soil Mechanics and Foundations Division, 98(12), 1311–1324. doi:10.1061/jsfeaq.0001816.

[29] Nayak, N. V. (1983). Recent advances in ground improvements by stone column. Proceedings of Indian Geotechnical Conference, 21-24 December, 1983, Madras, India.

[30] Fattah, M. Y., Shlash, K. T., & Al-Waily, M. J. M. (2011). Stress concentration ratio of model stone columns in soft clays. Geotechnical Testing Journal, 34(1), 50–60. doi:10.1520/GTJ103060.

[31] Bowles, J. E. (1996). Foundation Analysis and Design, The McGraw-Hill Companies Inc., Singapore.

[32] Dhani, N., Gasruddin, A., Hartini, H., & Baride, L. (2021). Unconfined compressive strength characteristics of over boulder Asbuton and zeolite stabilized soft soil. Civil Engineering Journal, 7(1), 40-48. doi:10.28991/cej-2021-03091635.

[33] Nazariafshar, J., Mehrannia, N., Kalantary, F., & Ganjian, N. (2017). Bearing Capacity of Group of Stone Columns with Granular Blankets. International Journal of Civil Engineering, 17(2), 253–263. doi:10.1007/s40999-017-0271-y.

[34] Mohanty, P., & Samanta, M. (2015). Experimental and Numerical Studies on Response of the Stone Column in Layered Soil. International Journal of Geosynthetics and Ground Engineering, 1(3), 27. doi:10.1007/s40891-015-0029-z.

[35] Castro, J. (2017). Groups of encased stone columns: Influence of column length and arrangement. Geotextiles and Geomembranes, 45(2), 68–80. doi:10.1016/j.geotexmem.2016.12.001.

[36] Ambily, A. P., & Gandhi, S. R. (2007). Behavior of Stone Columns Based on Experimental and FEM Analysis. Journal of Geotechnical and Geoenvironmental Engineering, 133(4), 405–415. doi:10.1061/(asce)1090-0241(2007)133:4(405).

[37] Shahu, J. T., & Reddy, Y. R. (2011). Clayey Soil Reinforced with Stone Column Group: Model Tests and Analyses. Journal of Geotechnical and Geoenvironmental Engineering, 137(12), 1265–1274. doi:10.1061/(asce)gt.1943-5606.0000552.

[38] Ghazavi, M., & Nazari Afshar, J. (2013). Bearing capacity of geosynthetic encased stone columns. Geotextiles and Geomembranes, 38, 26–36. doi:10.1016/j.geotexmem.2013.04.003.

[39] Lee, D., Yoo, C., & Park, S. (2007). Model tests for analysis of load carrying capacity of geogrid encased stone column. The Seventeenth International Offshore and Polar Engineering Conference, 1-6 July, 2007, Lisbon, Portugal.

[40] Brooker, E. W., & Ireland, H. O. (1965). Earth Pressures at Rest Related to Stress History. Canadian Geotechnical Journal, 2(1), 1–15. doi:10.1139/t65-001.

[41] Sivakumar, V., & Black, J. (2007). A laboratory model study of the performance of vibrated stone columns in soft clay. 17th International Conference on Soil Mechanics and Foundation Engineering, Madrid, Spain.